COUPLED MODELING FOR INVESTIGATION OF BLAST INDUCED TRAUMATIC BRAIN INJURY

X. GARY TAN, ROBERT N. SAUNDERS AND AMIT BAGCHI

U.S. Naval Research Laboratory
Multifunctional Materials Branch
Washington, DC 20375, USA

Key words: Human Biomechanics, Blast, Traumatic Brain Injury (TBI), CSF, ALE, MPM.

Abstract. Modeling of human body biomechanics resulting from blast exposure is very challenging because of the complex geometry and the substantially different materials involved. We have developed anatomy based high-fidelity finite element model (FEM) of the human body and finite volume model (FVM) of air around the human. The FEM model was used to accurately simulate the stress wave propagation in the human body under blast loading. The blast loading was generated by simulating C4 explosions, via a combination of 1-D and 3-D computational fluid dynamics (CFD) formulations. By employing the coupled Eulerian-Lagrangian fluid structure interaction (FSI) approach we obtained the parametric response of the human brain by the blast wave impact. We also developed the methodology to solve the strong interaction between cerebrospinal fluids (CSF) and the surrounding tissue for the closed-head impact. We presented both the arbitrary Lagrangian Eulerian (ALE) method and a new unified approach based on the material point method (MPM) to solve fluid dynamics and solid mechanics simultaneously. The accuracy and efficiency of ALE and MPM solvers for the skull-CSF-brain coupling problem was compared. The presented results suggest that the developed coupled models and techniques could be used to predict human biomechanical responses in blast events, and help design the protection against the blast induced TBI.

1 INTRODUCTION

Blast events accounted for nearly 70% of injuries in wounded service members, and are the main cause of TBI [2]. Compared to impact-related injury, the mechanisms involved in blast injury are much less understood. Primary concussive blast injuries may be caused by the direct transmission of the blast wave across the cranium and the brain, by the impact of blast ejecta on the body (e.g., shrapnel and debris) and by the individual striking an object (e.g., a fall against ground or vehicle). Because of ethical reasons experimental neurotrauma is typically studied using either physical surrogates or animal models [4]. Direct use of animal model results to human is questionable as it is not clear how to reproduce the blast loads on humans in animals. The multi-physics computational models of injury biomechanics complemented with benchmark quality experiments may provide a foundation for better understating of injury mechanisms. Validated models could also be used for the design of improved protective equipment, injury diagnostics, casualty care and forensics [5].

Accurate simulation of blast waves impacting a human body and the resulting human biomechanical response is very challenging as it involves several physical and biomedical

disciplines as well as a range of spatial and temporal scales. A blast wave, interacting with human, transfers energy from the body surface into the interior. The overpressure on the body surface generates two types of waves with the body organs and tissues: pressure waves and shear waves. As the pressure wave traverses an organ such as brain or lung, it creates sharp pressure gradients on sensitive microstructures such as brain neurons. It propagates with specific tissue speed of sound and causes local wave diffractions/reflections on tissue interfaces with impedance differential creating compressive and tension strain responses. Most biological materials are weaker in tension than in compression and thus disruption and therefore damage at the tissue interface may occur. When the pressure wave compresses a gas containing structure such as an alveolus or bowel segment, the subsequent expansion causes damage to the wall of the structure. Shear waves propagate within the body with much slower speed, last much longer and cause larger tissue deformations. The tension and shear waves as well as asynchronous movements of tissues with differing inertia may cause tearing of structures from their attachments and shearing of solid organs. The musculoskeletal system being solid is relatively resistant to the pressure waves while initial shock waves of sufficient intensity may cause long bone fracture [7]. Because of these, the inclusion of whole human body (skin, skeleton, and organs) is important to accurately account for the propagation and spatial distribution of stress waves inside the human body and to predict the complicated dynamic tissue/organ responses to the blast loading.

To simulate the blast-induced human body biomechanics, we developed a whole human body anatomic geometry/mesh model and the FEM biomechanics model. This human body model can be used to simulate the blast wave loading on the body surface, the biomechanical response of the body interior as well as the body biodynamics [10]. A mesh with the maximum element size less than three millimeters was used to resolve the smallest stress wavelength, small geometric features and material interfaces within the human body. The high-fidelity CFD model was used to simulate the interaction between the human body and the blast wave generated by a C4 explosion. Both Eulerian and ALE methods was used and compared for the high explosive burn simulation. The blast pressure loads computed during the CFD analysis are applied to the human body finite element model for biomechanics simulations. Using the human FEM model we investigated the brain biomechanics including the coup-contrecoup phenomena and the injury probability in the brain. The coupled gas dynamics and biomechanics solutions have been validated against the recent shock tube testing data on the physical phantom and animal [11].

For the closed system such as the human head, the interaction between the nearly incompressible CSF and the surrounding tissue is very strong at the fluid-solid interface during the impact [6]. A small change in the fluid volume by the tissue deformation will lead to an excessive flow pressure exerting to the neighboring tissue and thus is very difficult to solve. The Eulerian-Lagrangian coupling approach is computationally expensive in the iterative two-way coupling process and may not converge at all. To be more efficient and numerically stable, we employed both ALE method and MPM method [9] to solve such problem. In ALE, the motion and deformation of all materials are solved in the Lagrangian step, the distorted CSF mesh is then smoothed to preserve the mesh quality, and finally the solutions in the CSF and at the fluid-solid interface are conservatively transferred from the old mesh to the new one. The particle based MPM method has the potential to be another unified approach since both fluid dynamics and solid mechanics are solved simultaneously in the

Lagrangian description. We compared the accuracy and efficiency of both the ALE and the MPM in the skull-CSF-brain coupled problem.

2 METHODS

We describe the computational models and methods for simulating blast wave interaction with a human body and the associated biomechanical response. Several FSI coupling approaches for modeling injury caused by blast wave and impact loads are discussed.

2.1 High-Fidelity Human Model of a Human Body

The human computational models are based on the geometry of a 3D male anatomy model by the Zygote Media Group, Inc. The anatomy model starts with an entire skeleton model based on CT scans, and upon which all the other systems (e.g., skin, organs) fit together.

The generated hexahedral mesh consists of four different materials, i.e. brain with spinal cord, lung, skeleton and tissue for the rest of body. The outer surfaces of different body parts are shown in Figure 1a. The average element size is 2.5mm. The total number of elements is over 4.2 million. The mesh for the CFD simulation of a human standing on the rigid ground was also constructed as shown in Figure 1b, where an octree mesh was used to discretize the air domain between the human body and the outer boundaries. The smaller cell size (2.5mm) near human body is used and total number of cells is about 14 million. The computational meshes generated for these simulations are of good quality and can use relatively large time step sizes without resorting to the artificial time scaling treatment.

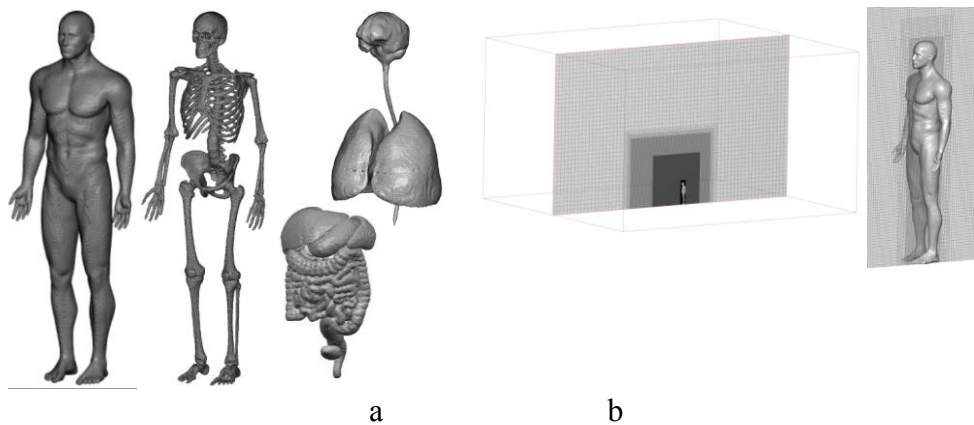
a   b

Figure 1. Computational models from Zygote geometry. a) Skin surface, skeleton and lungs, brain, spinal cord and organs underneath skin of FEM mesh, b) CFD mesh for blast interacting with human body and a close-up view of CFD mesh around human body.

Table 1. Mechanical properties used in human FE model [13].

Tissue	Material	Constants	Mass Density Kg/m3
Skeleton	Linear elastic	E=5GPa, v=0.3	1100
Brain, spinal cord	Viscoelastic	K=2.19GPa, G_0=49KPa, G_1=33KPa, τ=6ms	1000
Lung	Linear elastic	E=50Kpa, v=0.3	100
Tissue	Linear- elastic	E=80MPa, v=0.4	1000

We used homogenized material properties for different part of human body as listed in Table 1. The brain and spinal cord was modeled as an isotropic viscoelastic material, without considering the difference between white mater and grey mater. The CSF layer between the skull and the brain was not explicitly modeled but was considered to be part of the brain. The lungs were modeled as separated organs because of the sound speed being much slower in the lung than in other body tissues. All materials other than skeleton, brain and lungs were modeled as soft tissues in which an elastic material was assumed.

2.2 CFD Model of Blast Physics

For accurately capturing the detailed shock wave phenomena around the solid object, we use the CFD method to solve governing equations of the physics laws, i.e., conservation of mass, momentum, and energy. Consider the inviscid compressible Navier-Stokes equations

$$\frac{\partial U}{\partial t} + \nabla \cdot \mathbf{F} = 0 \tag{1}$$

where $U = \{\rho, \rho\mathbf{v}, \rho E\}^T$ and ρ, $\mathbf{v}$, E are the density, the velocity and the total energy and $\mathbf{F}$ is the flux. The equation of state (EOS) and the total energy of ideal gas are as below

$$p = \rho RT, \quad \rho E = \frac{p}{\gamma - 1} + \frac{1}{2}\rho\mathbf{v} \cdot \mathbf{v} \tag{2}$$

where R is the ideal gas constant, T is the temperature, and γ is the adiabatic index.

The high explosive is commonly modeled by the Jones-Wilkins-Lee (JWL) EOS

$$p = A(1 - \frac{\omega\rho}{R_1\rho_0})e^{-R_1\frac{\rho_0}{\rho}} + B(1 - \frac{\omega\rho}{R_2\rho_0})e^{-R_2\frac{\rho_0}{\rho}} + \omega\rho e \tag{3}$$

The material constants are in Table 2. The detonation velocity is used for the calculation of ignition time at the given location of explosive. The intrinsic energy per unit mass e is related to the total energy E by $e = E - (\mathbf{v} \cdot \mathbf{v})/2$. The JWL equation is reduced to the ideal gas law when the density ρ is much smaller than the initial density ρ_0.

Table 2. Mechanical properties in JWL EOS for the explosive charge.

A (GPa)	B (GPa)	R_1	R_2	ω	e_0 (MJ/Kg)	ρ_0 (Kg/m^3)	V_D (m/s)
373.8	3.747	4.15	0.9	0.35	3.68	1630	6930

Both the ALE and the Eulerian methods are employed to solve the above equations. The ALE method involves three-step solution: Lagrangian, remeshing, and advection steps. The equation (1) in the Lagrangian description becomes

$$\rho\frac{D\mathbf{v}}{Dt} + \nabla \cdot (p\mathbf{1}) = 0, \quad \rho\frac{De}{Dt} + p\nabla \cdot \mathbf{v} = 0 \tag{4}$$

which can be readily solved by the explicit FEM solver. Among different remeshing methods to smooth the distorted mesh, we relocate the nodes by solving an elastic solid deformation problem using the implicit FEM solver

$$\nabla \cdot \boldsymbol{\sigma} = 0 \tag{5}$$

along with the prescribed displacement boundary condition and a zero-stress initial condition.

For the advection step, the current solution ϕ such as $\rho, \rho\mathbf{v}, \rho E$ at each element is transported from the old mesh to the new mesh by the convective velocity $\mathbf{c}$

$$\frac{\partial \phi}{\partial t} + \mathbf{c} \cdot \nabla \phi = 0 \tag{6}$$

To maintain the numerical stability and conserve the mass, linear momentum and energy, we use the upwinding process in which the calculation of gradient depends on the direction of the convective velocity $\mathbf{c}$ and only uses the information from the upstream direction. The nodal velocity was calculated from the new elemental linear momentum using the shape functions. The nodal acceleration was updated from the equilibrium with new state variables.

For the Eulerian approach, the discontinuous Galerkin (DG) method was used to obtain the weighted residual form to (1) for each control volume/cell. The finite volume method is recovered with a constant weighting function in the DG method. We adopted the HLLC solver [14] for the flux calculation. The explicit method was used for the resulting semi-discrete system, of which the first-order forward Euler scheme is particularly efficient and provides a sufficient accuracy for the current applications. For both the Euler method and the advection step of ALE method, the second-order accurate solution was obtained by a piece-wise linear data reconstructions. The limiter function was used to eliminate the spurious oscillations.

2.3 Blast Induced Human Biomechanics

In the blast-human interaction process, the blast duration is very short (a few milliseconds) and during the blast loading the induced human body motion is small (a few centimeters). The one-way (explicit) coupling of flow and biomechanical analyses, in which the blast wave influences the body but the body movement does not influence the blast wave, is sufficient and much more efficient compared to the tightly coupled fluid-structure interaction (FSI) scheme (see, e.g., [1]). In this approach, the blast simulation was first carried out by assuming a rigid stationary human body. The time histories of the flow over-pressures and the corresponding locations are recorded. In the subsequent biomechanical analysis, we apply the overpressure loadings to the closest facet on human body surface for each time step. The force resulting from the flow over-pressure on each face of solid surface is computed by

$$\mathbf{F} = -p\mathbf{n}A \tag{7}$$

in which p is the overpressure, $\mathbf{n}$ and A are the face normal pointing away from solid and the face area respectively.

For the short-term event such as the blast wave interacting with human body, we choose the explicit finite element solver using the brick element with reduced integration. The hourglass control was used to effectively suppress artificial hourglass modes and meanwhile minimize the nonphysical stiffening of response. The numerical stability was inspected by the total energy balance of kinetic energy, internal energy and external work.

2.4 Head Skull-CSF-Brain Coupling Model

There are two main approaches for simulation of FSI problems: 1) Monolithic approach such as ALE method to solve the flow and the structure simultaneously; 2) partitioned approach to solve the flow and the structure separately. In a typical mesh-based partitioned

approach, the flow problem is solved by the Eulerian CFD solver and the structural problem is solved by Lagrangian FEM solver. The deformation in the fluid mesh due to the motion of fluid-structure interface is solved by the remeshing. With the relaxation of either the deformation to the fluid or the flow pressure to the structure at the interface, the flow and structural interaction is solved successively until the change in the solution is smaller than the convergence criterion. For the closed head with nearly incompressible CSF, the convergence using such approach is very difficult to achieve.

The ALE method is less complicated and more stable than the partitioned method for the closed-head FSI problem. The ALE method solves the CSF flow and the tissue deformation simultaneously. In the Lagrangian step, the Tait EOS is used for the CSF

$$p = \frac{\kappa}{n}[(\frac{\rho}{\rho_0})^n - 1]$$

(8)

where κ =2.2GPa, n =7.15. The density and linear momentum in the CSF are advected from the distorted mesh to the new mesh after the remeshing step. The nodal velocity and acceleration in the CSF and at the CSF-tissue interface are then updated for the next Lagrangian step.

A meshless method such as material point method (MPM) is another monolithic FSI method. With the MPM, the Lagrangian material points are used to discretize both fluid and solid. The interaction of the material points is calculated on a fixed background grid on which the momentum equation is solved. Different from other particle based methods, the evaluation of interpolation functions and derivatives relies on the background grid and does not involve the costly neighbor search. Compared to the ALE method, the remeshing and the advection are not needed. Since material points carry the mass and the history-dependent variables, the numerical diffusion associated with the advection is avoided.

3 RESULTS

For the blast and the biomechanics simulations, we used the multi-physics code CoBi, written in C++ and run on both Windows and Linux cluster. The implementations were verified and validated extensively through many related applications [11,12].

3.1 Modeling of Explosive

A spherical TNT charge with radius of 0.05 m is considered at the center of the model and surrounded by the air. A 1.134° conical model with radius of 0.5m was built in which hexahedral elements with elemental length of 0.001m in the radial direction were used. The detonation starts at the center of charge, and the detonation front is moved with the given velocity of detonation. An element detonates if the detonation front reaches this element. From this time the JWL-equation turns on for this element. The surrounding air uses the same EOS with a different starting density and internal energy.

Both the ALE method and the Eulerian method were used for the high explosive burn simulation for the time duration of 0.1 msec. Both methods conserves the mass (=15.138mg) in the simulations. In terms of energy conservation, the Eulerian method conserves the total energy (=31.676KJ) precisely while the ALE method cannot conserve the energy. Figure 1 show that the mass density ρ, flow velocity $\mathbf{v}$ and flow pressure p propagating along the radial direction at 0.1ms. Compared to the Eulerian method the ALE method is much more diffusive

and thus is less accurate. The solution of $\{\rho, \rho\mathbf{v}, \rho e\}$ along the radius at the end of Eulerian simulation was saved into a file and used as the initial condition in the 3-D simulation of blast loading on the human.
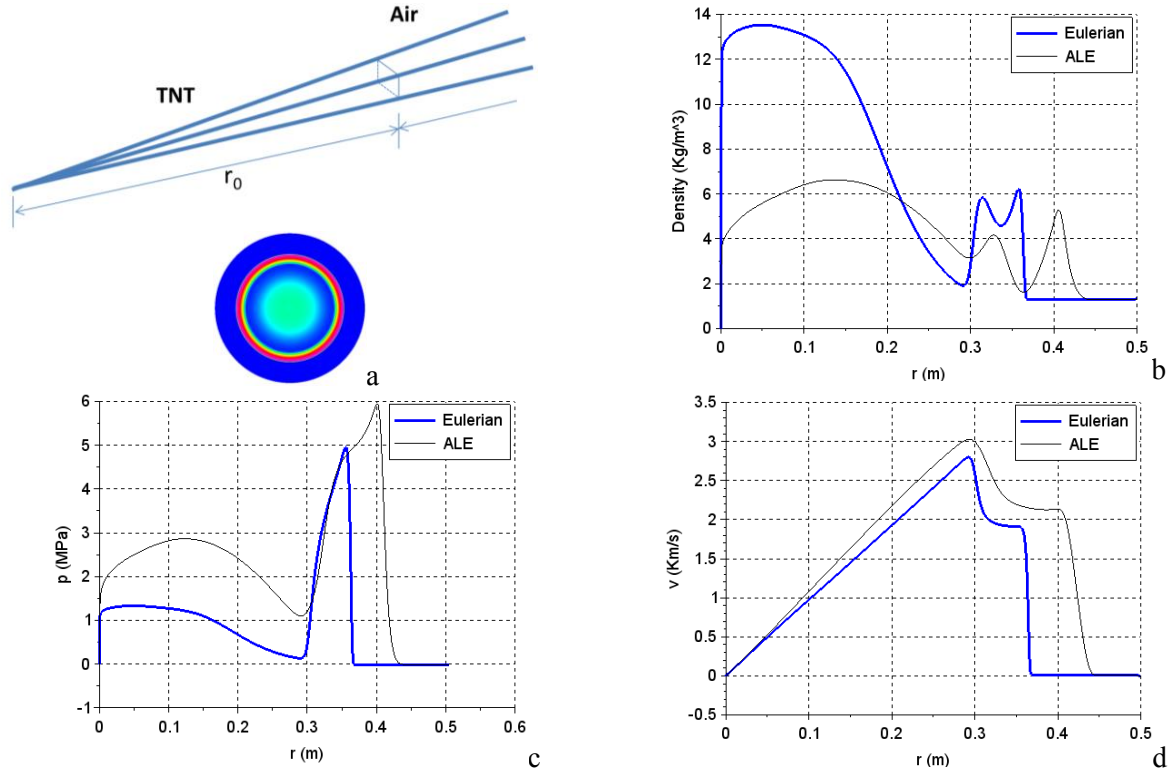

Figure 2. a) Conical model for TNT-air blast simulation with r_0=0.05m and pressure contour at 0.1ms; b) density, c) pressure, d) velocity along radial direction at 0.1ms between ALE and Eulerian methods.

3.2 Blast Loading on Human Body

The explicit flow solver was used to simulate the blast wave induced overpressure field around the human body. The human is facing the explosion. The 5lb C4 explosive is located at 92 inch away from the human body and 50 inch above the ground. The open boundary condition is applied at the outer boundaries. The time step size is about 0.1 micro-sec and the time duration of simulation is 12ms. The developed 1-D and 3-D simulation strategy [13] was used in which the conical model simulated the initial explosion stage before reaching the ground. The 3D simulation was then restarted by using the radial solution as the initial condition.

The results of the blast interaction with the stationary human body surface are shown in Figure 3. The shock front has been captured reasonably well. It takes just a few milliseconds for the blast wave to pass through the human body. After that the pressure field around the human goes back to the ambient and the resultant forces on the human body diminish rapidly. The Mach stem forms and progresses due to the reflection from the presence of ground and the human body. The pressure loading at each time step was saved into a file.

The calculated pressures on the head surface have a sharp rise and experience both positive and negative phases. The reflected pressure peak at forehead is much higher than other

468

locations. The calculated pressure at the rear portion of head surface is higher than the temple, because of the diffraction of the shock front. The peak pressure at the temple is similar to the incident peak pressure. The ground reflection reaches the forehead at 4.8ms.
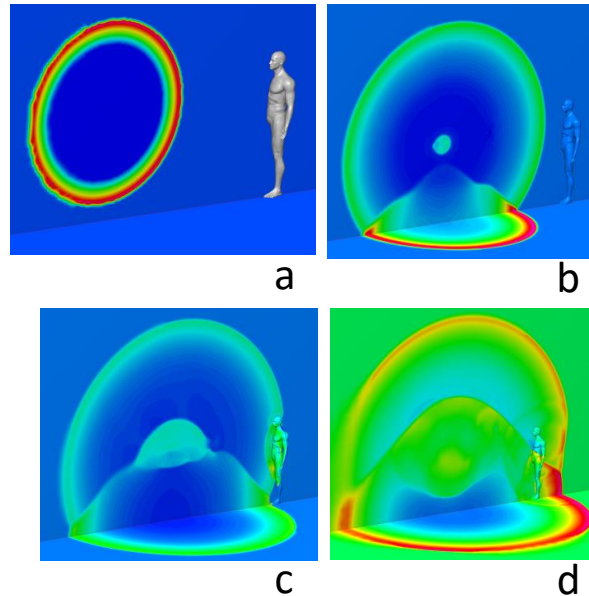

Figure 3. Blast simulation of C4 explosion interacting with human body. a) Initial pressure field from 1D simulation at 0.45msec, b) simulation shows ground reflection at 1.45ms, c) overpressure on human at 2.45ms, d) overpressure on human at 3.95ms.

3.3 Biomechanics Response of Human under Blast Loading

By applying the computed blast loading to the human skin, we simulated the biomechanical response of the human body for 12ms. The time step size is 0.08 micro-sec. In the human body dynamics, the effect of gravity was ignored and no consideration was given to the frictional contact interaction between the human body and the ground.

As shown in Figure 4, in the first few milliseconds the moving shock front diffracts on the human body surface, and reflects around concave regions (eye socket, lower neck, and groin). The blast pressure reaches the face and the chest first since they are closer to the explosive. The high pressure on the lower leg was caused by the ground reflection. The high-amplitude stress wave propagated inside the human body prior to any visible displacement of human body. Figure 4 shows the pressure in two sagittal planes. A stiff material like the skeleton has the higher pressure, while the pressure in a softer material like the lung is much lower. The pressure contours on both surfaces of skeleton and brain at several time instances are shown in Figure 5. Since the explosion occurs in front of the human, the blast wave first reaches the chest and front lobe of the brain. After the blast wind has passed, the human body does not move much and the maximum displacement is a few centimeters, which justifies the one-way coupling strategy for the simulation of blast-human body interaction. The numerical results of brain pressure response are qualitatively similar to the experimental data obtained in [3], in which an elliptical object is subjected to the shock wave loading generated from the shock tube. Several phenomena observed in the testing data during the first 2.5 millisecond were also occurred in the numerical simulation: 1) there was about a 0.1 millisecond time delay of

pressure onset between coup and contrecoup sites, 2) the negative pressure occurred first in the contrecoup site, 3) the positive peak pressure in the contrecoup site was higher than the coup site, 4) at the contrecoup site three positive peaks are gradually weakening, and 5) three negative pressure dips occurred over the cavitation limit of -100kPa.
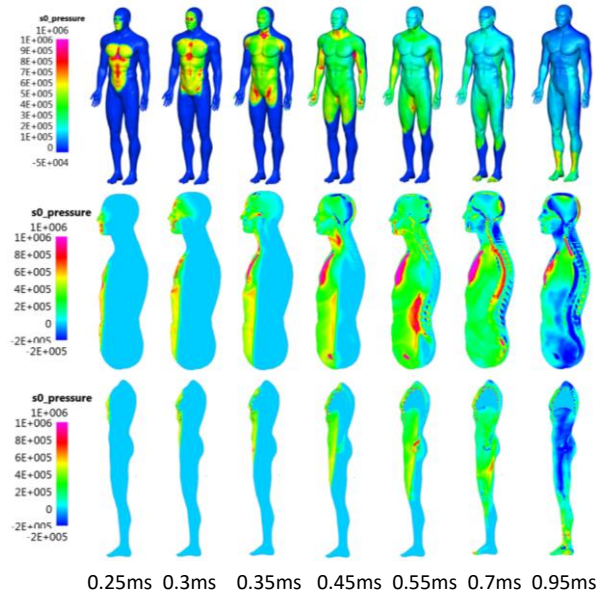

Figure 4. Human biomechanics under blast loading. Blast loading on human skin (top row); Pressure propagation in the middle sagittal plane (middle row); Pressure propagation in the para-sagittal plane (bottom row) at different times. Time offset by 1.8 ms between explosion CFD and FEM simulations.
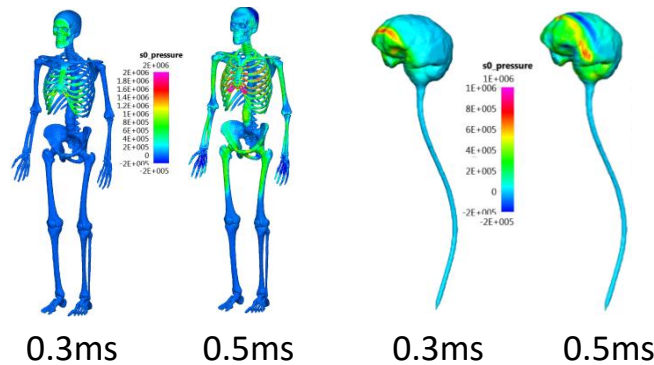
Figure 5. Pressure propagation in skeleton and brain at different times of human body under C4 explosion. Time offset by 1.8 ms between explosion CFD and FEM simulations.

3.4 Modeling of Skull-CSF-Brain Interaction

For the closed-head impact, the interaction between the CSF and the surrounding tissue is strong and difficult to model. We explore both ALE and MPM methods to solve such problem. In Figure 6, the head model with a simplified geometry and high-quality fine mesh was used to simulate the skull-CSF-brain interaction during the impact. Assume the head has been accelerated to the initial velocity of 3m/s after the blast loading and is colliding with a rigid wall. The commonly used partitioned FSI solving approach is unstable for this strong

coupling problem. In the ALE model, the CSF layer was modeled as the ALE fluid and other materials as the Lagrangian solid. In the MPM model, all materials were modeled as Lagrangian particles and a 0.002m uniform background grid was used. The cubic B-spline basis function was used to reduce the grid-crossing errors.
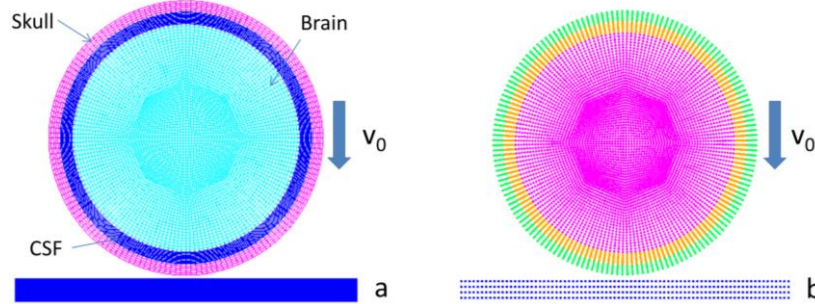

Figure 6. Head model for skull-CSF-brain interaction using ALE method (a) and MPM method (b).

The total simulation time is 5ms and the time interval for remeshing and advection is 20 micro-sec. At 4.36 ms, the head starts to rebound. In Figure 7, the maximum negative pressure in CSF is -236KPa and occurs at 0.92 ms. After 2.18 ms, the pressure in the brain and CSF stays in positive because of the compressed intracranial volume. Compared to the pressure, the shear strains which can cause the injury are developed at the later time (Figure 8). The maximum shear occurs at the CFS-skull and CSF-brain interfaces because the CSF has no shear resistance. Figure 9 shows that the CSF flows around the brain and the flow speed in CSF is in the same level of initial impact speed. At the end of 5ms, the CSF flows upward. With the implemented ALE method we are able to further simulate the CSF-tissue interaction for the closed-head injury during the impact, using an anatomic head model and a robust remeshing technique.
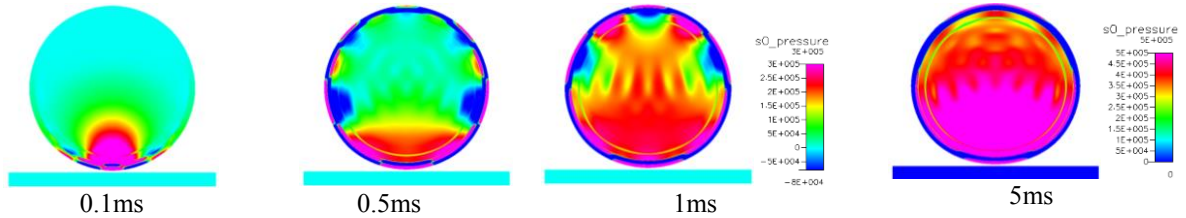

Figure 7. Skull-CSF-brain coupled solution using ALE model. Pressure at t=0.1ms, 0.5ms, 1ms, 5ms.
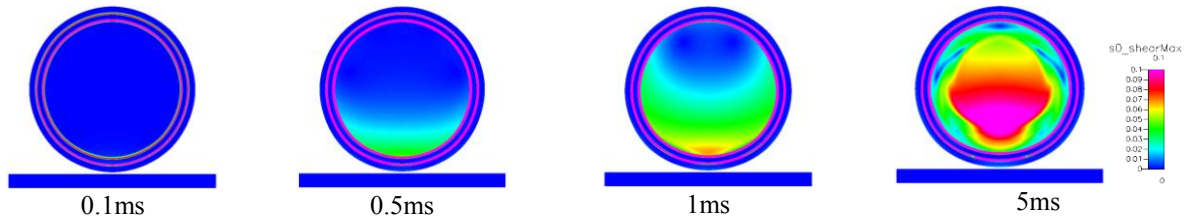
Figure 8. Skull-CSF-brain coupled solution using ALE model. Shear strains at t=0.1ms, 0.5ms, 1ms, 5ms. Maximum shear strains occur at CSF-brain and CSF-skull interfaces.
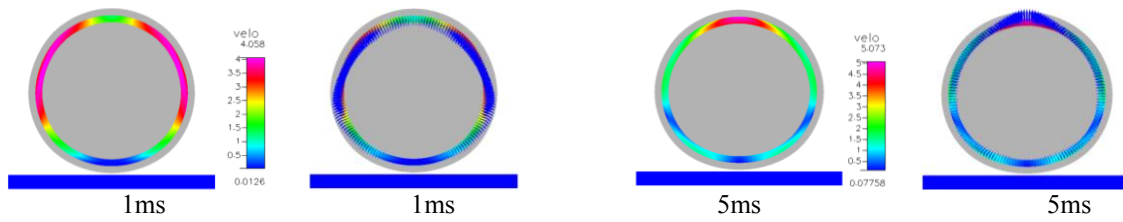
Figure 9. Skull-CSF-brain coupled solution using ALE model. Flow velocity magnitude and direction in CSF at t=1ms, 5ms.

Figure 10 shows the results when solving the same problem using the MPM. The MPM model behaves softer than the ALE model and yields larger contact area between the skull and the wall. Compared to the ALE model, the magnitude of pressure is much higher in the CSF and much lower in the brain. Like in other particle based methods, it is difficult to compute the particle mass density/pressure accurately for the nearly incompressible material under large deformation. To remedy it, the adaptive MPM to resample the particles or treating the evolution of pressure implicitly [8] becomes necessary to obtain the solution with similar accuracy as the ALE method in the skull-CFS-brain interaction problem.
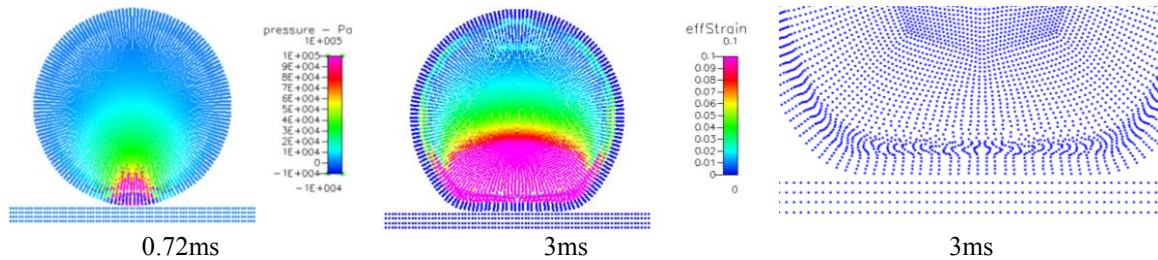

Figure 10. Skull-CSF-brain coupled solution using MPM model. a) pressure at 0.72ms, b) strain at 3ms, c) zoom-in of contact area showing movement of material points in CSF at 3ms.

4 CONCLUSIONS

This paper presented the methods to model the blast-induced human biomechanics and injury. Several coupling approaches were implemented for modeling human body injury caused by IED blast wave and fragmentation/impact loads. The computational methods and simulation results of blast injury mechanisms were described. In modeling the explosive the Euler solver performs much better than the ALE solver since the Eulerian solver conserves the energy precisely. Our computational studies have shown that the disparity of spatial and temporal scales of the problem justifies simplifying assumptions for various phases of blast human injury simulations. The human body can be assumed as rigid for simulations of the blast wave propagation around the body to compute body loading as inputs for biodynamics and biomechanics simulations. For the strong coupling problems of skull-CSF-brain interaction under impact the ALE method solves it with a reasonable response. For the same problem the MPM needs more improvements such as solution adaptation and energy conserving scheme to achieve the similar performance as the ALE method.

The presented coupling framework provides a foundation for a better understanding of blast injury mechanisms, and also for the development of personal protective armor. Several challenges remain, such as better material properties for high strain rate tissue biomechanics, CSF cavitation, accurate models of IED induced penetrating injury, and model validation.

ACKNOWLEDGEMENT

REFERENCES

[1] Badia, S., Nobile, F., Vergara, C. Fluid-structure partitioned procedures based on robin transmission conditions, *Journal of Computational Physics* (2008) 227:7027-7051.

[2] Eskridge, S.L., Macera, C.A., Galarneau, M.R. et al. Injuries from combat explosions in Iraq: injury type, location, and severity. *Injury* (2012) 43(10):1678–1682.

[3] Goeller, J., Wardlaw, A., Treichler, D., O'Bruba, J., Weiss, G. Investigation of Cavitation as a Possible Traumatic Brain Injury (TBI) Damage Mechanism from Blast, *J. Neurotrauma* (2012) 29(10):1970–1981.

[4] Goldstein, L.E., Fisher, A.M., Tagge, C.A. et al. Chronic traumatic encephalopathy in blast-exposed military veterans and a blast neurotrauma mouse model. *Sci. Trans. Med.* (2012) 4(134):134-160.

[5] Gupta, R.J. and Przekwas, A.J. Mathematical models of blast induced TBI: current status, challenges and prospects, *Frontiers in Neurotrauma* (2013) 4:59.

[6] Halabieh, O., Wan, W.L. Simulating mechanism of brain injury during closed head impact, F. Bello, E. Edwards (Eds.): *ISBMS* (2008), LNCS 5104, 107–118.

[7] Hull, J.B. An investigation into the mechanism of traumatic amputation by explosive blast. Doctor thesis, *University of Birmingham* (1995).

[8] Jiang C. The material point method for the physics-based simulation of solids and fluids, Doctor Thesis, *University of California, Los Angeles* (1995).

[9] Sulsky, D., Chen, Z. and Schreyer, H.L. A particle method for history-dependent materials, *Computer Methods in Applied Mechanics and Engineering* (1994) 5:179–196.

[10] Tan, X.G., Kannan R., Przekwas A.J., Ott K., Harrigan, T., Roberts, J. and Merkle, A. An enhanced articulated human body model under C4 blast loadings, *ASME Int. Mech. Eng. Congress and Exposition* IMECE 2012-89067 (2012).

[11] Tan X.G., Przekwas, A.J., Long, J.B. Validations of virtual animal model for investigation of shock/blast wave TBI, *ASME Int. Mech. Eng. Congress and Exposition* IMECE 2013-64587 (2013).

[12] Tan, X.G. and Przekwas A.J. A computational model for articulated human body dynamics, *Int. J. of Human Factors Modeling and Simulation* (2011) 2:85-110.

[13] Tan, X.G., Kannan R. and Przekwas A.J. A Comparative study of the human body finite element model under blast loadings, *ASME Int. Mech. Eng. Congress and Exposition*, IMECE2012-89072 (2012).

[14] Toro, E.F., Spruce, M. and Speares, M. Restoration of the contact surface in the HLL-Riemann solver, *Shock Waves* (1994) 4:25–34.